Disease Models & Mechanisms 4, 649-658 (2011) doi:10.1242/dmm.006775

Unbound (bioavailable) IGF1 enhances somatic growth

Sebastien Elis[1,*], Yingjie Wu[1,*], Hayden-William Courtland[1], Dara Cannata[1], Hui Sun[1], Mordechay Beth-On[1], Chengyu Liu[2], Hector Jasper[3], Horacio Domené[3], Liliana Karabatas[3], Clara Guida[3], Jelena Basta-Pljakic[4], Luis Cardoso[4], Clifford J. Rosen[5], Jan Frystyk[6] and Shoshana Yakar[1,‡]

SUMMARY

Understanding insulin-like growth factor-1 (IGF1) biology is of particular importance because, apart from its role in mediating growth, it plays key roles in cellular transformation, organ regeneration, immune function, development of the musculoskeletal system and aging. IGF1 bioactivity is modulated by its binding to IGF-binding proteins (IGFBPs) and the acid labile subunit (ALS), which are present in serum and tissues. To determine whether IGF1 binding to IGFBPs is necessary to facilitate normal growth and development, we used a gene-targeting approach and generated two novel knock-in mouse models of mutated IGF1, in which the native *Igf1* gene was replaced by Des-*Igf1* (KID mice) or R3-*Igf1* (KIR mice). The KID and KIR mutant proteins have reduced affinity for the IGFBPs, and therefore present as unbound IGF1, or 'free IGF1'. We found that both KID and KIR mice have reduced serum IGF1 levels and a concomitant increase in serum growth hormone levels. Ternary complex formation of IGF1 with the IGFBPs and the ALS was markedly reduced in sera from KID and KIR mice compared with wild type. Both mutant mice showed increased body weight, body and bone lengths, and relative lean mass. We found selective organomegaly of the spleen, kidneys and uterus, enhanced mammary gland complexity, and increased skeletal acquisition. The KID and KIR models show unequivocally that IGF1-complex formation with the IGFBPs is fundamental for establishing normal body and organ size, and that uncontrolled IGF bioactivity could lead to pathological conditions.

INTRODUCTION

Insulin-like growth factor-1 (IGF1) plays a pivotal role in fetal development, growth and tissue homeostasis. *Igf1*-null mice have marked growth retardation in utero and weigh 65% of normal weight at birth (Baker et al., 1993; Liu et al., 1998). Postnatally, *Igf1*-null mice do not undergo a peri-pubertal growth spurt and weigh only 30% of adult wild-type animals. These mice are infertile, indicating that IGF1 plays an essential role in the reproductive system. IGF1 receptor (*Igf1r*)-null mice are 45% the weight of controls at birth and die shortly thereafter owing to organ hypoplasia (Baker et al., 1993), identifying IGF1R as the main mediator of IGF1 bioactivity. IGF1, together with insulin and growth hormone (GH), regulate glucose, lipid and protein metabolism, and thereby regulate body composition. IGF1 is also involved in the regulation of innate and acquired immunity, in wound healing and tissue repair, as well as in cognitive functions (for reviews, see Yakar et al., 2005a; Yakar et al., 2005b; Yakar et al., 2002b).

IGFs are bound to IGF-binding proteins (IGFBPs), which modulate the actions of IGFs, facilitate their storage in extracellular matrices and determine the net IGF bioactivity (Baxter, 2000; Mohan and Baylink, 2002). Previous studies were unable to determine whether IGF1 binding to IGFBPs at tissue sites is in fact necessary to facilitate normal growth, development and/or metabolism. To date, six high-affinity IGFBPs have been characterized (Baxter, 2000; Mohan and Baylink, 2002). Recent studies have demonstrated that IGFBP levels vary depending on exercise (Wakai et al., 2009), surgery and pregnancy (Forbes and Westwood, 2008), nutrition (Kaaks, 2004), and age (Frystyk, 2005), and that the levels of the various IGFBPs are regulated by different hormones in serum and other biological fluids. Studies in mice lacking the different IGFBPs show modest deficiencies in somatic growth (10-20% decreases in body weight), which are mostly attributable to decreased IGF levels in serum and IGF stability in tissues (Ning et al., 2006). A triple knockout of IGFBP3, IGFBP4 and IGFBP5, the main IGFBPs present in serum, results in an only 22% reduction in body weight, despite 65% decreases in serum IGF1 levels compared with wild type (Ning et al., 2006). Similarly, gene inactivation of the acid labile subunit (ALS), which stabilizes the binary complex of IGF1 and IGFBP3 or IGFBP5, results in an approximate 10-20% decrease in body weight (Courtland et al., 2010; Yakar et al., 2009b). In our previous study we generated a triple-knockout mouse with liver IGF1 deficiency (LID) and null alleles of the *Igfals* and *Igfbp3* genes (LAB mice). Body weights of LAB mice, followed from 3 to 16 weeks of age, were reduced by ~20% as compared with control mice, despite undetectable levels of IGF1 in serum (Yakar et al., 2009b). In that study, however, we also found that genetic ablation of *Igfbp3* (which produced only 40% reductions in serum IGF1) led to a ~15% increase in body weight (Yakar et al., 2009b). A study published by Stratikopoulos et al. (Stratikopoulos et al., 2008) demonstrated that serum IGF1

[1]Division of Endocrinology, Diabetes and Bone Disease, Mount Sinai School of Medicine, New York, NY 10029, USA
[2]Transgenic Core Facility, National Heart, Lung, and Blood Institute, National Institutes of Health, Bethesda, MD 20892, USA
[3]Endocrinology Research Center, Division of Endocrinology, R. Gutierrez Children's Hospital, 1425 Buenos Aires, Argentina
[4]Department of Biomedical Engineering, The City College of New York, New York, NY 10031, USA
[5]Maine Medical Center Research Institute, 81 Research Drive, Scarborough, ME 04074, USA
[6]The Medical Research Laboratories, Clinical Institute of Medicine, and Medical Department M (Diabetes and Endocrinology), Aarhus University Hospital, Aarhus 8000, Denmark
*These authors contributed equally to this work
‡Author for correspondence (shoshana.yakar@mssm.edu)

Received 5 September 2010; Accepted 18 April 2011

contributes to determining approximately 30% of the adult body size, providing additional support to the previous studies showing that marked reductions in serum IGF1 lead to only a ~20% decrease in body weight. Together, these studies support the notion that IGFBPs serve as reservoirs that release the ligand, and control IGF action in serum and local microenvironments.

The solution-structure of IGF1 has been solved by nuclear magnetic resonance (NMR) (Cooke et al., 1991; Sato et al., 1993). In conjunction with IGF mutagenesis studies, the interaction of IGF1 with IGFBPs was revealed and this led to the description of two IGF analogs that have a large reduction in affinity for the IGFBPs but retain normal affinity for IGF1R: these analogs are R3-IGF1 (Coolican et al., 1997; Flint et al., 1994; McCusker et al., 1998) and Des1-3-IGF1 (Des-IGF1) (Ballard et al., 1987; Ballard et al., 1988; Ross et al., 1989; Szabo et al., 1988). The R3-IGF1 mutant has a Glu (E)-to-Arg (R) substitution at position 3 of the IGF1 peptide, and Des-IGF1 has a three-amino-acid truncation at the N-terminus. Both mutants have several times lower affinity for IGFBP3 than native IGF1 and show greatly reduced binding to all other IGFBPs (Bayne et al., 1989; Gillespie et al., 1990; King et al., 1992; Lemmey et al., 1991).

The aim of the present study was to determine how unbound (bioavailable) IGF1 affects somatic growth and skeletal acquisition, as well as tissue integrity and body composition. To that end we generated two mouse models of knock-in R3-IGF1 (KIR) and Des-IGF1 (KID), in which genes encoding mutant IGF1 replaced the endogenous *Igf1* gene and were expressed under the endogenous *Igf1* promoter. These models offer significant advantages over other models of an impaired IGF1 axis, allowing the study of the autocrine effects of IGF1 independent of the IGFBPs. These mouse models represent an artificial situation in which IGF1 is found in an unbound form and, thus, its post-translational control is impaired and its bioactivity is increased. In this study we describe the first characterization of KIR and KID mice during growth and development.

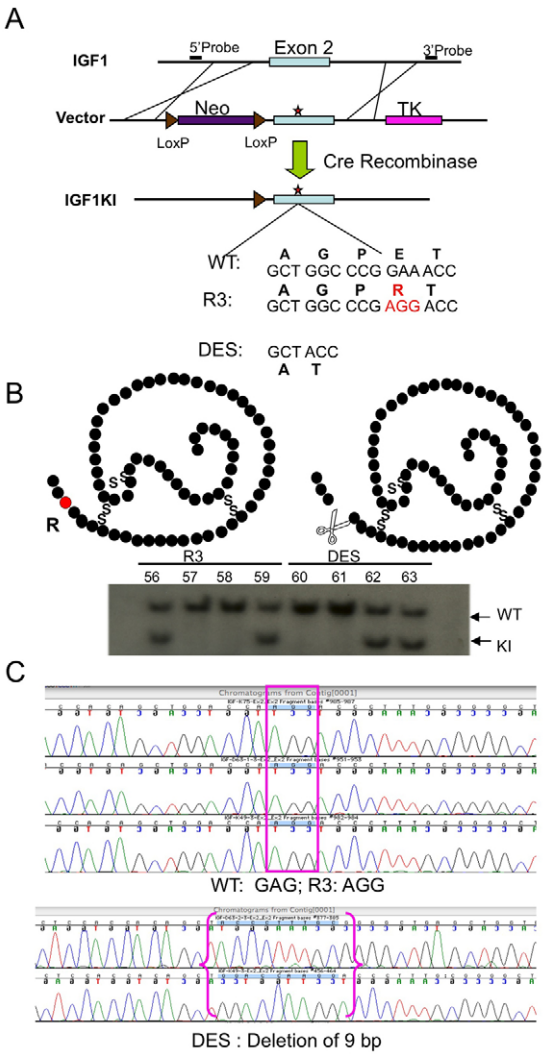

Fig. 1. Knock-in strategy. (A) Schematic representation of the targeting construct, in which the two mutations in exon 2 were introduced, adjacent to a *neo* cassette flanked by two *loxP* sites (used for selection). The *neo* cassette was subsequently removed using the Cre transgene. (B) Southern blot analysis was used to identify embryonic cell mutant clones (knock-in; KI). Above the blot we present a schematic of the mutated peptides. (C) Sequence analysis confirmed the mutations. WT, wild type.

RESULTS

Generation of mutant IGF1 mouse models using the knock-in strategy

The generation of the two new mouse models of mutated IGF1 was based on extensive in vitro studies with a variety of cell lines as well as on in vivo models whereby these mutants were injected or overexpressed. The first mutant has an amino acid substitution of E to R at position 3 and was therefore named knock-in R (KIR). The second mutant has a deletion of the first three amino acids of IGF1 (Des-IGF1) and was therefore named knock-in D (KID). Both IGF1 mutant peptides have similar affinity for IGF1R as does the wild-type IGF1 peptide. However, these two mutants have several times lower affinity for IGFBP3 than natural IGF1 and have greatly reduced binding to other IGFBPs. KIR and KID mutations were introduced separately into the mouse genome by a knock-in technique (Fig. 1); therefore, the mutated IGF1 molecule is expressed under its natural promoter (and the regulation of the *Igf1* promoter is not affected). The two target constructs were injected into mouse embryonic stem (ES) cells (C57BL/6J strain). The targeting constructs included a negative selection marker [herpes simplex virus (HSV) thymidine kinase (TK)] and a positive selection marker, i.e. neomycin (Neo) resistance. When genetic recombination occurred in the correct genetic loci, the TK marker was removed and only the *neo* cassette and the introduced mutated *Igf1* were incorporated into the genome. The neomycin cassette was removed by crossing the founder mouse lines with EIIa-Cre transgenic mice, in which Cre-recombinase is expressed at the two- to four-cell stage.

KID and KIR mice show impaired regulation of the GH-IGF1 axis, leading to decreased ternary complex formation in serum

Serum IGF1 levels in KID and KIR mice were assessed by commercially available radioimmunoassay (RIA) kits using polyclonal antibody. Using this assay we found marked reductions in serum IGF1 levels at 4, 8 and 16 weeks of age (Fig. 2A) in both KID and KIR mutants compared with controls. However, these

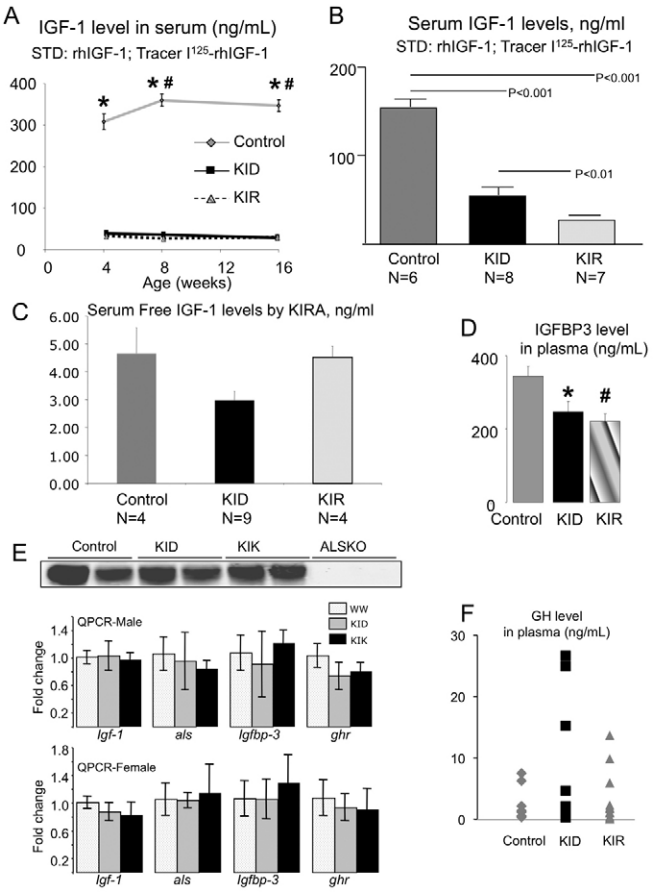

Fig. 2. KID and KIR mice show significant decreases in serum IGF1 and IGFBP-3 levels, and increases GH levels. (A) Serum IGF1 levels determined at 4, 8 and 16 weeks of age by RIA (ALPCO) were significantly lower in KID and KIR mice as compared with controls (*n*=5 per age and genetic group). (B) Serum IGF1 levels determined at 8 weeks of age by RIA (NIH) were significantly lower in KID and KIR mice as compared with controls. (C) Serum free IGF1 levels determined by KIRA. (D) Serum IGFBP3 levels from 8-week-old female KID and KIR mice were decreased compared with controls (*n*=5-12 per genetic group). (E) Serum ALS levels as measured by western blot (*n*=5 in each group) and expression levels of *Igf1*, *Als*, *Igfbp3* and *Ghr* genes in livers from control, KID and KIR mice at 8 weeks of age. (F) Serum GH levels from 8-week-old female KID and KIR mice were increased compared with controls (*n*=5-12 per genetic group). Data presented as mean ± s.e.m.; *P*<0.05 was considered statistically significant (* denotes significance between control and KID; # denotes significance between control and KIR).

reductions might reflect reduced assay sensitivity. Therefore, we measured recombinant R3-IGF1 and Des-IGF1 at known concentrations using the same RIA. We found that, at low concentrations (<150 ng/ml), the precision of the kit was 70% for Des-IGF1 but only 6% for R3-IGF1 (supplementary material Fig. S1). We therefore used a different RIA using the NIH polyclonal antibody (developed by Albert F. Parlow, National Hormone and Peptide Program, CA), which recognizes the IGF1 mutants. We performed assays using Des-IGF1 for the standard curve and as a tracer, wild-type IGF1 for the standard curve and as a tracer, and a combination of the two (detailed in supplementary material Fig. S1). In both assays we found that KID mice have 60% reductions in total IGF1 levels in serum (Fig. 2B) compared with wild type, and KIR mice showed even further reductions.

Next we looked at the bioactivity of free IGF1 in serum, using a cell-based IGF1 kinase receptor activation (KIRA) bioassay (Chen et al., 2003), which determines the ability of serum to stimulate IGF1R in vitro. Because serum is compared with a serial dilution of recombinant human IGF1 (rhIGF1), it is possible to express the obtained results in mg/l. The KIRA results contrasted with those obtained by immunoassay, because the KIRA bioassay yielded levels of bioactive IGF1 of similar magnitude in each of the three groups, although some statistical differences were observed (Fig. 2C). Because sera obtained from KID mice exhibited IGF1 bioactivity similar to that of control sera (by KIRA assay), we believe that the concentration of Des-IGF1 that we measured using the above RIA mostly represents the fraction of Des-IGF1 mutant that was bound to the IGFBPs (with lower affinity than wild type).

Serum levels of IGFBP3, the main binding protein of IGF1 in serum, decreased significantly (~40%) in both KID and KIR mice (Fig. 2D), suggesting decreased IGF1 binding to IGFBP3 and reduced IGFBP3-IGF1 binary complex formation in serum. Lastly, we measured ALS levels in serum from control and mutant mice by western blot assay and found no significant changes between the groups (Fig. 2E). Expression levels of the *Igf1*, *Igfals* or *Igfbp3* genes in the liver were assessed by real-time PCR and showed no differences between the groups in both genders (Fig. 2E).

Consequently, by using ^{125}I-IGF1 (Yakar et al., 2009b), we examined the ability of serum from KID and KIR mice to support the formation of ternary complexes. In this assay, the tracer ^{125}I-rhIGF1 is used to displace the 'cold' (i.e. endogenous) IGF1 bound to IGFBPs in serum samples. This assay provides qualitative information about the presence of all three components that are routinely seen in serum IGF1-binding ternary complexes (IGF1, a binding protein and ALS). Importantly, the percent binding seen in the different fractions does not reflect an absolute concentration of any of the compounds in serum. As seen in Fig. 3A, when rhIGF1 was used as a tracer, ternary complex formation (fractions 0-10) was largely reduced in sera from KID and KIR mice, suggesting significant reductions in the levels of IGFBPs, as shown before (Fig. 2D). However, IGF binary complexes (fractions 20-30) were present in KID and KIR sera. This reflects the fact that Des-IGF1 as well as R3-IGF1 has lower affinity for the IGFBPs than does wild-type IGF1, allowing more ^{125}I-rhIGF1 to displace the 'cold' mutant IGFs in serum. When ^{125}I-Des-IGF1 was used as tracer (Fig. 3B), we could not detect any binary or ternary complex formation in sera from control mice (Fig. 3B). This reflects the fact that ^{125}I-Des-IGF1 has a much lower affinity for the IGFBPs than does wild-type IGF1 and therefore was not able to displace the 'cold' wild-type IGF1 in serum (from control mice) (Fig. 3B). Using ^{125}I-Des-IGF1 with serum from KID mice revealed the presence of binary and ternary complexes (Fig. 3B), reflecting a greater displacement of 'cold' Des-IGF1 (found in sera from KID mice) with ^{125}I-Des-IGF1.

Introduction of the KID and KIR mutation did not affect the *Igf1* promoter region. Mutant *Igf1* expression levels in liver and muscle did not differ significantly from controls (data not shown). However, because IGF1 levels in serum were reduced dramatically, we examined GH levels in serum (Fig. 2F). We found that, at 8 weeks of age, both KID and KIR female mice showed an increase in the mean serum GH levels, probably owing to reduced serum

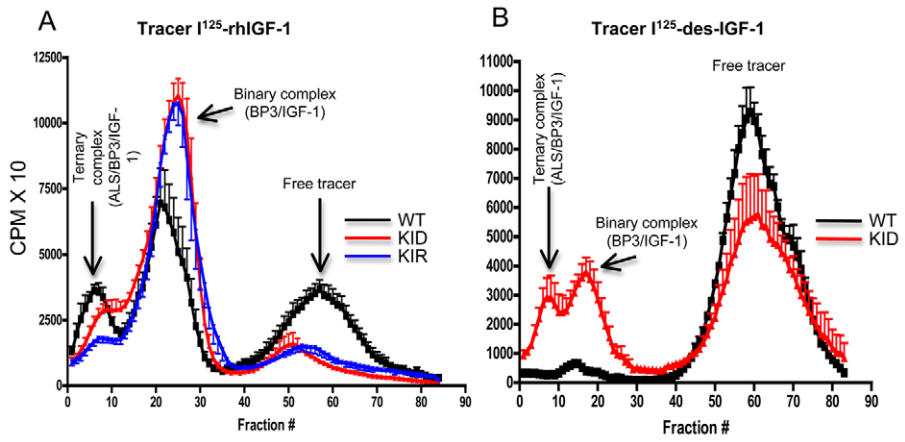

Fig. 3. Profiles of ternary complex formation in sera from control, KID and KIR mice. Each profile represents six mice. (A,B) Complex formation using I^{125}-rhIGF1 (A) or I^{125}-Des-IGF1 (B) as a tracer. CPMX10, counts per minute × 10; WT, control (wild type).

IGF1 levels and an impaired inhibitory-feedback mechanism. However, this observation must be taken cautiously because GH levels were measured only once per mouse.

Unbound (bioavailable) IGF1 increases body size and affects relative organ growth

Body weights of KID and KIR mice (Fig. 4A) were significantly increased from 4 to 16 weeks of age as compared with controls in both genders. Likewise, both KID and KIR mice showed increased body length at 4, 8 and 16 weeks of age (Fig. 4B). Body composition, assessed by NMR, revealed that, at 16 weeks of age, relative lean mass (fat-free mass) in female and male KID and KIR mice increased as compared with controls (Fig. 4C). By contrast, whereas, in control mice, body adiposity increased with age (Fig. 4D), in KID and KIR mice relative body adiposity decreased in both genders. Likewise, the relative weights of gonadal fat pads in KID and KIR mice were significantly lower than in controls (Table 1).

Unbound (bioavailable) IGF1 increases mammary gland complexity and stimulates uteral growth

We found that relative weights of livers, hearts and brains of KID and KIR mice did not differ significantly from controls. By contrast, we found that the relative weights of kidney, pancreas and spleen increased in KID and KIR mice at all ages studied (Table 1).

Transgenic mice with localized mammary gland overexpression of Des-human-IGF1 (Des-hIGF1), created using the whey acidic protein (WAP) promoter, demonstrate incomplete mammary involution and ductile hypertrophy (Hadsell et al., 1996). To determine the impact of free IGF1 on mammary gland development in KID and KIR mice, we analyzed female mammary glands at 4, 8 and 16 weeks of age. Interestingly, mammary glands of KIR and KID mice showed a greater degree of complexity as compared with control mice at all ages analyzed (Fig. 5). Glands from 16-week-old KID and KIR mice demonstrated a 56.3% and 70.4% increased complexity over control mice, respectively (P<0.001).

In addition to the mammary ductal phenotype, KID and KIR mice possess uterine defects. Uterus from KID and KIR mice were twofold larger than those of controls and appeared to be hyperplastic. Histological examination revealed that, in KID and KIR mice, the epithelial height is increased and cell layers are disorganized. The uterus stroma in KID and KIR mice appeared fibrotic, and the size of the myometrial layer was increased (Fig. 6). Despite the aforementioned phenotype, KID and KIR female mice can support embryonic development and litter size is not affected.

Unbound (bioavailable) IGF1 promotes linear growth and skeletal acquisition, and leads to robust bones

To understand how free IGF1 affects cortical and trabecular bone architecture we dissected femurs from 16-week-old female mice and analyzed them using microcomputed tomography (micro-CT; Table 2). Our data revealed that free IGF1 in KIR female mice promoted large increases in total cross-sectional area (Tt.Ar.), cortical bone area (Ct.Ar.), cortical thickness (Ct.Th.), polar moment of inertia (J_o), robustness (Tt.Ar./length) and marrow area (Ma.Ar.). Cortical changes were less pronounced in KID mice and consisted only of significant increases in Ct.Ar., Ct.Th. and J_o. Tissue mineral density (TMD) did not differ significantly between control and KID or KIR mice. However, KIR mice had significantly reduced TMD as compared with KID mice. To determine whether changes in morphology and composition altered mechanical properties, femora from 16-week-old female KID and KIR mice were subjected to four-point bending. We found that both KID and KIR mice tended to have increased stiffness as compared with controls, but these values did not reach statistical significance. However, maximum load was significantly greater in KIR mice as compared with both KID and control mice.

Trabecular architecture, assessed at the distal femur, showed that the bone volume/total volume fraction (BV/TV) increased markedly in KID mice as well as in KIR mice (borderline marked significance) when compared with controls (Table 2). This increase resulted from a significant increase in trabecular number (Tb.N.) in both KID and KIR mice, and a consequent decrease in trabecular spacing (Tb.Sp.) in KID and KIR (borderline significant) mice. There were no statistically significant differences in trabecular thickness (Tb.Th.) or TMD when comparing strains.

In agreement with the micro-CT data, we found that the bone formation marker osteocalcin was elevated significantly in KIR mice, whereas KID mice did not differ from controls (Table 2).

DISCUSSION

Using a gene-targeting approach we generated two novel knock-in IGF1 mutant models, in which the native *Igf1* gene was replaced

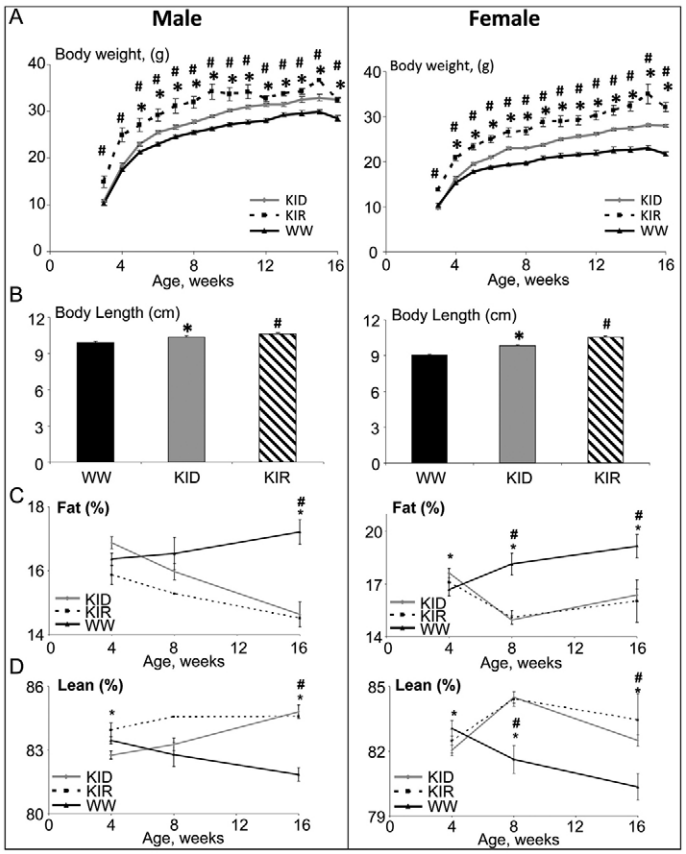

Fig. 4. Free IGF1 increases body weight, body length and lean mass and decreases body adiposity in both male and female mice. (A) Body weight was followed weekly. Both KID and KIR mice show a significant increase in body weight as compared with controls (n=10 to 20 per age and genetic group). (B) Body length (nose to anus), measured at 16 weeks of age, increased significantly in KID and KIR mice (n=10 per age and genetic group). (C,D) Body composition assessed by NMR revealed a significant increase in lean (fat-free) mass in both KID and KIR mice (D), whereas fat mass significantly decreased (C) (n=10 per age and genetic group). x-axis represents weeks. Data are presented as mean ± s.e.m.; P<0.05 was considered statistically significant (* denotes significance between control and KID mice; # denotes significance between control and KIR mice). WW, control (wild-type) mice.

Table 1. Relative weights of organs dissected from 16-week-old female mice

Organ	Control (n=10)	KID (n=14)	KIR (n=11)
Liver	4.52±0.09	3.90±0.12[a,c]	4.37±0.11[c]
Gonadal fat	1.63±0.15	0.81±0.14[a]	0.66±0.14[b]
Pancreas	0.76±0.06	1.18±0.07[a,c]	0.82±0.04[c]
Spleen	0.37±0.02	0.39±0.01[c]	0.50±0.03[b,c]
Kidney	1.27±0.03	1.58±0.03[a,c]	1.42±0.03[b,c]
Muscle (quadriceps)	0.87±0.09	0.47±0.02[a]	0.54±0.02[b]
Lung	1.00±0.13	0.86±0.06	0.87±0.06
Brain	1.71±0.09	1.60±0.04	1.55±0.07
Heart	0.50±0.03	0.52±0.02	0.57±0.02
Uterus and ovaries	0.64±0.06	1.17±0.09[a]	1.14±0.08[b]
Mammary gland	0.88±0.07	0.54±0.04[a]	0.61±0.08[b]

[a]KID different from control (P<0.05).
[b]KIR different from control (P<0.05).
[c]KID different from KIR (P<0.05).
Percentages relative to body weight are shown.

by Des-IGF1 (KID) or R3-IGF1 (KIR). We demonstrated that IGF analogs are more potent in increasing somatic growth than native IGF1 in vivo, and this is tissue specific and independent of serum IGF1 levels. Although these are two artificial mouse models, studying their phenotype enhanced our understanding of the biology of IGF1 in tissues.

Reductions in serum IGF1 levels in KID and KIR mice are consistent with data showing reduced stability of those analogs in serum (Ballard et al., 1991; Bastian et al., 1993; Francis et al., 1990), in particular with the observation that recombinant Des-IGF1 injected into nude mice was rapidly cleared from serum and distributed to tissues (Ballard et al., 1991; Sun et al., 1997). It is important to note that serum IGF1 levels in KID and KIR mice were similar to those reported for LID, IGFBP3 knockout (IGFBP3KO) or ALS knockout (ALSKO) mice (Yakar et al., 2009b). Reduced serum IGF1 levels in KID and KIR mice correlated with reduced serum IGFBP3 levels, probably owing to reduced IGF1-IGFBP3 complex formation and rapid degradation of the latter. Serum IGFBP3 concentrations in KID and KIR mice were similar to those found in LID mice with low levels of IGF1 and normal levels of the ALS protein (Yakar et al., 2009b). By contrast, ALSKO mice, which also have decreased serum IGF1 levels, exhibit markedly reduced serum IGFBP3 (Yakar et al., 2009b), supporting the notion that binding of ALS to IGFBP3 (and not IGF1 to IGFBP3) is an important factor in determining IGFBP3 stability in serum. In humans, total ablation of the *IGF1* gene (reported in one patient) did not alter serum IGFBP3 (Woods et al., 1996). However, in humans, IGFBP3 also binds IGF2, which stabilizes it in serum, whereas, in the mouse, IGF2 is not detectable in serum postnatally. Because *Igfals* gene expression in KID and KIR mice is intact, we did not expect a dramatic decrease in IGFBP3 levels in serum. In the present study, we also found that the ability of the two IGF1 mutants to form ternary complexes of IGF1-IGFBP3-ALS in serum was dramatically reduced, resembling the phenotype of ALSKO mice (Yakar et al., 2009b). However, unlike ALSKO mice, which exhibited mild growth retardation, KID and KIR mice showed increased growth, implying that IGF1 bioactivity in tissues was increased. It is important to note that, despite reductions in total IGF1 levels in the serum of KID and KIR mice, we did not find changes in free IGF1 levels in the serum between the groups. Thus, our studies refer to the role of free IGF1 in tissues; the biological significance of free IGF1 in serum is not yet resolved.

Similar to our previous observations with LID mice (Yakar et al., 2001; Yakar et al., 2004), the decreases in serum IGF1 in KID and KIR mice resulted in increased serum GH levels. These elevations result from a feedback loop between serum IGF1 and the pituitary. However, despite extensive experimentations trying to understand the nature of this loop, it is yet unknown what form of IGF1 (ternary complex, binary complex or free) feeds back to the pituitary. In ALSKO or IGFBP3KO mice, despite decreases in serum IGF1 levels, we could not detect increases in serum GH in both male and female mice from 4 to 16 weeks of age. Similarly,

Table 2. Skeletal traits of femurs isolated from 16-week-old female mice

Trait	Control (*n*=9)	KID (*n*=12)	KIR (*n*=11)
Body weight (g)	22.65+1.32	27.08+2.14[a]	32.10+3.56[a]
Body length (cm)	9.26+0.30	9.83+0.19[a]	10.55+0.33[a]
Femur length (mm)	15.65+0.19	16.26+0.61[a]	16.75+0.59[a]
Cortical bone traits (micro CT, femoral mid-diaphysis)			
Tt.Ar.	1.95+0.18	2.12+0.21	2.49+0.32[a]
Ct.Ar.	0.84+0.06	0.94+0.04[a]	1.08+0.11[a]
Ma.Ar.	1.11+0.13	1.17+0.19	1.41+0.24[a]
Ct.Th.	0.19+0.01	0.2+0.01[a]	0.21+0.02[a]
RCA (Ct.Ar./Tt.Ar.)	0.43+0.02	0.45+0.04	0.44+0.04[a]
J_o	0.34+0.05	0.43+0.05[a]	0.6+0.1[a]
Robustness (Tt.Ar./length)	0.12+0.01	0.13+0.01	0.15+0.02[a]
TMD	1.31+0.03	1.36+0.04	1.29+0.08
Trabecular bone traits (micro CT, distal femur)			
BV/TV (%)	7.14+1.40	9.35+2.12[a]	9.27+1.40[a]
Tb.Th. (mm)	0.055+0.00	0.055+0.00	0.054+0.00
Tb.N. (1/mm)	1.30+0.20	1.70+0.30[a]	1.70+0.20[a]
Tb.Sp. (mm)	0.25+0.03	0.21+0.04[a]	0.19+0.02[a]
Mechanical testing (four-point bending assay)			
Stiffness (N)	152.5+6.5	163.9+4.3	164.4+7.6
Max stress (N)	25.58+0.85	27.55+0.55	31.60+1.56[a]
Bone formation marker			
Osteocalcin (ng/ml)	121.75+4.87 (*n*=4)	128.80+7.86 (*n*=5)	167.75+10.66[a] (*n*=4)

[a]Different compare with control (*P*<0.05).
RCA, relative cortical area.

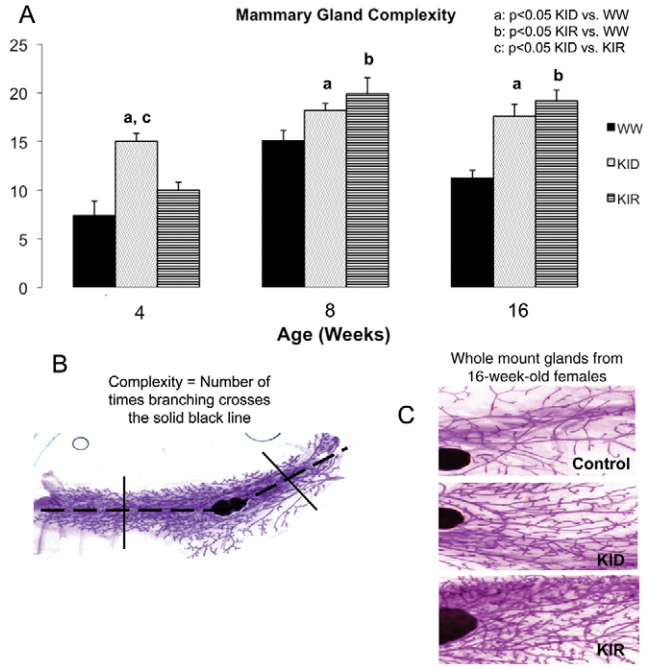

Fig. 5. Mammary gland morphology in control, KID and KIR female mice. (A) Mammary gland complexity was measured in female control, KID and KIR mice at 4, 8 and 16 weeks of age (for all groups, *n*=3-10 at 4 weeks of age, *n*=10-16 at 8 weeks of age and *n*=12-20 at 16 weeks of age). Differences between groups were measured by one-factor ANOVA. Values are presented as the mean ± s.e.m. *P*<0.05 was considered statistically significant. WW, control (wild-type) mice. (B) Complexity is a measure of the extent of ductal branching and was quantified using MicroSuite Basic imaging software to determine the number of intersecting branches along a line drawn midway between the leading edge of the ducts and each side of the lymph node. Broken line indicates the central line across the mammary fat pad. (C) Representative images of inguinal mammary gland whole mounts dissected from 16-week-old female control, KID and KIR mice. The glands were spread on a microscope slide and fixed in Carnoy's solution (60% absolute ethanol, 30% chloroform, 10% glacial acetic acid) for 2-4 hours. The fat pads were then hydrated in graded ethanol solutions and placed in Carmine Alum stain overnight. They were then dehydrated in graded ethanol solutions and finally placed in xylene prior to mounting with Mount-Quick mounting medium.

IGFALS-deficient humans, in which serum levels of IGF1 reduce dramatically, do not always show elevations in serum GH (Domene et al., 2009). Indeed, these data from the mouse models and the human counterparts raise new questions regarding the IGF-GH feedback regulation. Overall, we cannot exclude the possibility that the increases in GH levels together with increased IGF1 bioactivity of the analogs are in fact responsible for increased growth.

Unlike LID mice, which had a body size similar to controls up to ~10 weeks of age and then started to fall off the curve, KID and KIR mice showed increased body growth even up to 16 weeks. In LID mice we did not detect any increases in tissue IGF1 in response to GH elevations and, because body size did not differ from controls, we speculated that tissue IGF1 bioactivity was comparable. By contrast, although tissue *Igf1* gene expression did not differ between controls and KID or KIR mice, both mutants showed increased body size, again suggesting increased IGF1 bioactivity in tissues.

Strikingly, assessments of body composition by NMR showed increased lean (fat-free) mass in KID and KIR mice. However, this increase in lean mass was not reflected in the weight of the quadriceps (Table 1), which in fact exhibited decreased relative weight as compared with controls. The decrease in muscle weight in KID and KIR mice might result from muscle-type-specific effects of the IGF1 analogs, or uncoupling between muscle mass gain and body weight gain in KID and KIR mice. Those possibilities will have to be evaluated in future studies. Also, examinations of the KID and KIR models together with models of sarcopenia or muscle cachexia will give us a better insight into the role of bioactive IGF1 in maintaining muscle integrity under extreme conditions.

Fat content, by contrast, was decreased in both KID and KIR mice. It is conceivable that these alterations resulted from increased IGF1 bioavailability in adipose tissue. These observations are consistent with previous data in humans showing that IGF1 promotes increases in fat-free mass (Butterfield et al., 1997; Crist and Hill, 1990; Thompson et al., 1995) and decreases in fat mass (Thompson et al., 1995). Alternatively, it is possible that elevations in serum GH levels resulted in increased lipolysis and subsequent decreases in fat mass.

Not all organs responded equally to the genetic modifications. We found that spleen, kidney and uterus relative weights increased in KID and KIR mice, whereas relative weights of liver, pancreas, lungs and brain did not differ from controls. These observations

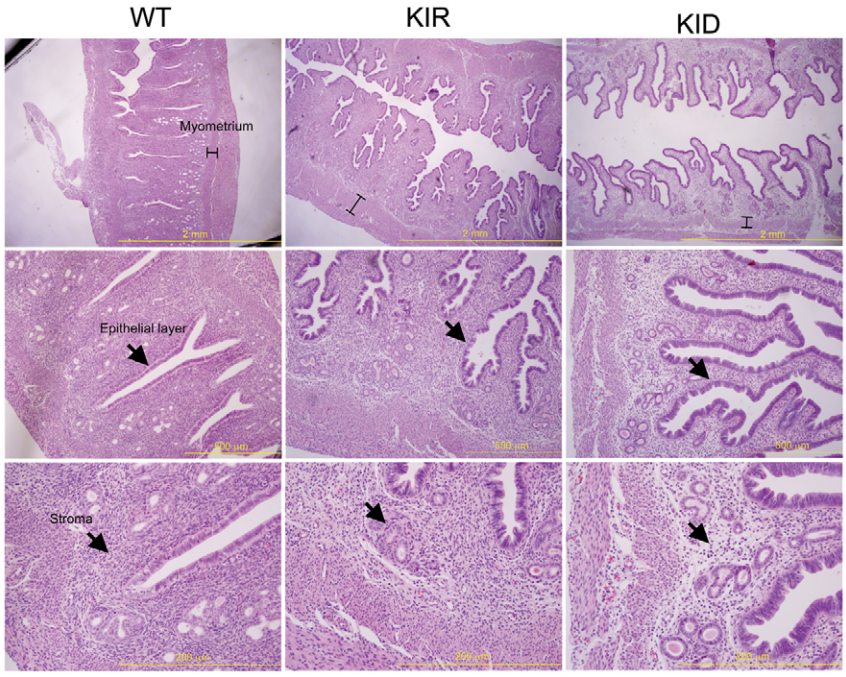

Fig. 6. Uterus histology in control, KID and KIR female mice. Images of uterus dissected from 16-week-old virgin female control, KID and KIR mice. (Top row) The myometrium height is indicated on sections stained with H&E. (Middle row) The uterine epithelial cell layer in KID and KIR mice is disorganized and the stroma layer (bottom row) exhibits fibrosis. Scale bars: 2 mm (top row); 500 µm (middle row); 200 µm (bottom row).

are consistent with previous findings in IGF1 transgenic mice, in which only selective organs responded to the high levels of IGF1 (Mathews et al., 1988). Also in agreement with previous publications, we found that free IGF1 enhanced mammary gland complexity and increased the uterine size in both KID and KIR mice. Together, these results suggest increased sensitivity of the female reproductive organs to IGF1 and this finding might be applicable to increased tumor incidence later in life.

Perhaps the most surprising data came from skeletal characterization of the KID and KIR mice. We found that free IGF1 in KIR mice promoted increases in all morphological bone traits, resulting in more robust, stronger bones when compared with controls. Interestingly, we found that KIR mice had a more profound phenotype than KID mice, the latter of which only showing enhancement of Ct.Ar. and thus the mathematically related traits Ct.Th. and J_o. This suggests that the KIR mutant protein is more potent than the KID mutant at skeletal sites. Specifically, the KIR mutant seems to enhance both periosteal apposition and endosteal resorption, as evidenced by significant increases in Tt.Ar. and Ma.Ar. Previous studies with animal models of serum IGF1 deficiency [LID (Yakar et al., 2009a), ALSKO (Courtland et al., 2010) or double-mutants LID/ALSKO mice (Yakar et al., 2006)] showed that reductions in serum IGF1 levels were associated with decreased bone accrual and with slender, mechanically inferior bones. By contrast, IGFBP3KO mice, which also show decreases in serum IGF1, exhibited a more robust bone phenotype when compared with controls (Yakar et al., 2009b). This was attributed in part to the growth-inhibitory effect of IGFBP3: this inhibition was released in *Igfbp3*-null mice, leaving free IGF1 to interact with its receptor. Our current study is in line with the data obtained from the IGFBP3KO mice, suggesting that the poor binding of the KID and KIR mutant IGFs to IGFBPs, not only in serum but, most importantly, at tissue sites, enhanced IGF1 action.

IGF and its binding proteins (IGFBPs) continue to attract attention as potential therapeutics for a wide range of disease-related complications and cancer. Understanding IGF1 biology is of particular importance, even apart from its role in mediating growth, because it plays key roles in cellular transformation, organ regeneration, immune function, aging, sarcopenia, cachexia and skeletal growth. The KID and KIR models show unequivocally that IGF1-complex formation with the IGFBPs is fundamental for establishing normal body and organ size. These models, although artificial, represent useful tools to study the contribution of free IGF1 to physiological growth and pathological states.

METHODS

Animals

All mice were on the C57BL/6 genetic background. Mice were housed four per cage in a clean mouse facility and fed a standard mouse chow (Purina Laboratory Chow 5001; Purina Mills) and water ad libitum, and kept on a 12-hour light-dark cycle. Animal care and maintenance were provided through the Mount Sinai School of Medicine AAALAC Accredited Animal Facility. All procedures were approved by the Animal Care and Use Committee of Mount Sinai School of Medicine.

Constructs used for the generation of knock-in mice

The 5.8-kb mouse *Igf1* gene fragments containing point mutation L3R or with the first three amino acids deleted (DES) at exon 2 (Fig. 1A) were generated by three rounds of special PCR with the Phusion DNA polymerase (Finnzymes) under the following conditions: 98°C for 2 minutes, 98°C for 10 seconds, 59°C for 30 seconds, 72°C for 150 seconds with 35 cycles then a following 10 minutes at 72°C and storage at 4°C. The mutations were confirmed by DNA sequencing. Fragments were cloned into pCR Blunt II-TOPO vector (Invitrogen). A conditional gene-targeting vector was constructed from this 5.8-kb *Igf1* gene by a novel recombineering

approach adapted from Liu et al. (Liu et al., 2003). Briefly, the 5.8-kb fragment from the above pCR Blunt II-TOPO construct was cut out by *Not*I and *Spe*I, then ligated to PL253 vector containing the thymidine kinase cassette. This subcloned genomic region was then modified in a targeting approach using the *neo* cassettes from the PL452 vector. A floxed *neo* cassette from PL452 was inserted to *Igf1* intron 1. The gene-targeting vector was tested for functionality by transformation into arabinose-induced SW106 cells and the *neo* cassette removed using arabinose-induced Cre-expressing SW106 cells, which leave behind only a single *loxP* site in *Igf1* intron 1. The conditional targeting vector was then linearized by *Not*I digestion and electroporated into B6/129 F1 hybrid ES (V6.5) cells using standard procedures. G418 (200 μg/ml)-resistant clones were analyzed by Southern blot hybridization, using external 5′ probes (Fig. 1A,B). Targeted clones were confirmed by DNA sequencing (Fig. 1C). The targeted clones harboring the *loxP*-flanked *neo* cassette were injected into C57BL/6 blastocysts using standard procedures. After conformation of germline transmission, mice were crossed to EIIa-cre transgenic mice (Jackson Laboratories #003724) to remove the *neo* cassette. The knock-in lines were backcrossed to C57BL/6J (Jackson Laboratories #000664) for seven generations and maintained by intercrossing homozygous knock-in mice.

Determination of serum hormones

Mice were bled through the mandibular vein and serum samples were collected at the indicated ages. Serum IGF1 (American Laboratory Products Company, Salem, NH) and, with RIA developed by Albert F. Parlow (National Hormone and Peptide Program), osteocalcin (American Laboratory Products Company) and insulin (Millipore, Temecula, CA) levels were determined using commercial RIAs as previously described (Pennisi et al., 2006; Yakar et al., 2002a; Yakar et al., 2004). Plasma IGFBP3 levels and GH levels (both Millipore) were determined using ELISA assays.

Determination of serum IGF1 ternary complex formation

The protocol was adopted from Baxter and Martin (Baxter and Martin, 1989). 100 μl serum samples were incubated overnight at 22°C with I^{125}-IGF1 (at a final concentration of 10 ng/ml), then cross-linked with disuccinimidyl suberate as reported before (Domene et al., 2004). Complexes were separated using HiPrep 16/60 Sephacryl S-200HR columns and 1 ml fractions were collected and counted.

Determination of serum bioactive IGF1

This assay was performed as previously described (Chen et al., 2003). In brief, serum samples (diluted 1:20) were incubated with transfected cells for 15 minutes at 37°C. Next, samples were aspirated, cells lysed and the crude cell lysates assayed for levels of phosphorylated (i.e. activated) IGF1Rs by a specific TR-IFMA as previously detailed (Chen et al., 2003). The serum signals were compared with those of a serial dilution of rhIGF1, calibrated against the rhIGF1 WHO International Standard preparation 02/254 (obtained from NIBSC, Hertfordshire, UK). The KIRA is relatively specific for IGF1 – IGF-2 and insulin cross-reactivity equals 12% and <1%, respectively – and it is also precise [within and between assay coefficient variances (CVs) average 7% and 15%, respectively].

Determination of serum ALS

Sera were diluted 1:4 with saline and subsequently separated on a 4-12% acrylamide gel and transferred to nitrocellulose. Membrane was blocked with LI-COR block solution (Lincoln, NE) and incubated overnight at 4°C with a goat anti-ALS antibody (R&D Systems, Minneapolis, MN). Following washing, the membrane was incubated with IRDye 800CW-donkey anti-goat antibody (LI-COR). Bound antibodies were detected by LI-COR Odyssey infrared imaging system.

Determination of body composition

Body adiposity was measured using a Bruker minispec NMR analyzer mq 10 in non-anesthetized mice (Bruker Optics, Woodlands, TX).

Micro-CT

The bone samples were scanned using a high-resolution SkyScan micro-CT system. Images were acquired using a 10 MP digital detector, 10 W power energy (100 KV and 100 μA) and a 0.5-mm aluminum filter. X-ray projections are generated from the sample each 0.3 degrees, obtaining 680 consecutive views with a 6.7-μm image pixel size. Five exposures by projection (1767-millisecond exposure time) were used to produce high-contrast low-noise images. A system alignment procedure and flat field calibration were performed prior the scanning sequence.

Trabecular and cortical regions were defined as positions along the long axis of the femur relative to the growth plate reference. The cortical region of interest was selected as ±1.5 mm in length from the mid-diaphysis of the bone. The trabecular metaphyseal region was selected as 3 mm in length from the distal growth plate towards the diaphysis.

A modified back-projection reconstruction algorithm (NRecon, V. 1.6.1.2) included in the SkyScan acquisition system was used to generate cross-section images from the planar X-ray projections. Throughout the reconstruction procedure, images were optimized using a standard postalignment compensation algorithm, eliminating misalignment artifacts. Images were also treated using a smoothing filter (kernel=1) with a Gaussian window, ring artifact correction (=15) and beam hardening correction (49%). All the reconstruction parameters were applied identically to all bone scans and to the calibration scan of the bone mineral density (BMD) rods, with the exception of the postalignment compensation.

Mechanical testing

Mouse femora from 16-week-old control, KID and KIR mice were tested to failure by four-point bending using a servohydraulic materials testing system (Instron, Canton, MA). This test was used to measure whole-bone stiffness and maximum load (strength). Femora were placed with the anterior surface down on two lower supports. The two lower and two upper supports were set apart by 6.35 and 2.2 mm, respectively. Loading was centered over the midshaft, at a displacement of 0.05 mm/second until failure. All mechanical properties were calculated from the load-displacement curves, as described previously (Jepsen et al., 2007).

Histology

Tissues were dissected from euthanized mice, fixed in 10% buffered formalin for 24-48 hours and embedded in paraffin blocks. 5-μm

TRANSLATIONAL IMPACT

Clinical issue

An imbalance in the tightly regulated levels of insulin-like growth factor-1 (IGF1) has been associated with various pathological conditions, including type 2 diabetes, cachexia, chronic inflammatory conditions (such as inflammatory bowel disease), obesity, and age-associated decline in mental and physical competence. In addition, it has long been thought that supplementation with free IGF1 (e.g. Des-IGF1) can enhance athletic performance. Owing to its central role in the regulation of cell survival, cell cycle progression and cell differentiation, an imbalance in the expression of IGF1 or its receptor, IGF1R, could lead to uncontrolled cell division and ultimately to malignant transformation. Indeed, increased levels of IGF1 and IGF1R have been documented in multiple types of human malignancy. Increased levels of IGF1 have also been reported in acromegaly (involving excess production of growth hormone) and are associated with organomegaly (enlargement of organs), osteoarthritis and colonic polyps. A better understanding of the role of IGF1 and IGF1R in normal and pathological conditions would increase our understanding of the wide range of diseases in which their expression is altered.

Results

In this study, the authors use a gene-targeting approach to generate two novel knock-in mouse models (referred to as KID and KIR strains) that allow them to assess the effect of free (unbound) IGF1 on growth and development. Both the KID and KIR mouse strains carry a different form of mouse IGF1 with a reduced ability to bind IGF-binding proteins (IGFBPs), leading to reduced concentrations of IGF1 in serum. Both strains of mice exhibit increased somatic growth, as indicated by increased body weight and increased body and bone lengths. In addition, the mice exhibit selective organomegaly of the spleen, kidney and uterus, enhanced mammary gland complexity, and increased skeletal acquisition. The phenotype of these two mouse strains suggests that increased IGF1 activity in tissues leads to uncontrolled growth.

Implications and future directions

Des-IGF1 is currently available for personal use and is sold to athletes for improvement of muscle anabolism. However, the long-term effects of taking supplements such as Des-IGF1 are not yet known. The KID and KIR mouse models characterized here will help to better understand the long-term effects of IGF1 supplementation as well as the potential impact of free IGF1 on neoplasia and health or lifespan. These initial studies suggest that Des-IGF1 might be useful in the treatment of human disorders associated with an imbalance in IGF1 levels, such as sarcopenia or muscle cachexia. Furthermore, the KID and KIR mouse models will enable future investigations of mechanisms of learning and memory that are controlled by IGF1 in vivo.

sections were cut and stained with hematoxylin and eosin according to standard procedures.

Gene expression studies

Total RNA from livers and bone marrow cultures was extracted (TRIzol, Invitrogen, Carlsbad, CA) and RNA integrity verified (Bioanalyzer-Bio Sizing 2100, Version A.02.12 SI292, Agilent Technologies). RNA samples (1 mg) were reverse-transcribed using oligo(dT) primers (Invitrogen) and quantitative real-time PCR performed following the manufacturer's instructions using the QuantiTect SYBR Green PCR kit (Qiagen, Valencia, CA) in ABI PRISM 7900HT sequence detection systems (Applied Biosystems, Foster City, CA). Each transcript in each sample was assayed three times and the fold-change ratios between experimental and control samples were calculated relative to β-actin.

Statistical analysis

All differences in mean serum hormones, organ weights, body composition and growth among the different groups were assessed by ANOVA. Values are presented as mean ± s.e.m.; $P<0.05$ was considered statistically significant.

All bone traits, body weight, body composition, serum hormones and micro-CT measurements are presented as means ± s.e.m. One-way analysis of variance (ANOVA) was used to test for differences among groups at each age (Statview software version 5.0, SAS Institute). If ANOVA revealed significant effects, the means were compared by Fisher's test, considering $P<0.05$ as significant.

ACKNOWLEDGEMENTS

Financial support was received from funding agencies in the United States: NIH Grants AR054919 (S.Y.), AR055141 (S.Y.); NIH/NIA AG034198 (L.C.), NIH/HLI HL101157 (L.C.) and NSF/MRI CBET-0723027 (L.C.); NIH/NIAMS AR53853 (C.J.R.), AR45433 (C.J.R.); and Argentina CONICET PIP 11420090100045 (H.J.). We thank Lone Kvist (Aarhus University Hospital, Norrebrogade 44, DK-8000 Aarhus C, Denmark) for helping with the KIRA assay.

COMPETING INTERESTS

The authors declare that they do not have any competing or financial interests.

AUTHOR CONTRIBUTIONS

S.Y. and Y.W. conceived and designed the experiments; S.E., Y.W., H.-W.C., D.C., H.S., M.B.-O. and C.L. performed experiments with the mouse models; H.J., H.D., L.K. and C.G. performed the ternary complex formation experiments; J.B.-P. and L.C. performed the mCT studies; J.F. performed the KIRA assay; C.J.R. performed RIAs; and S.Y. wrote the paper.

SUPPLEMENTARY MATERIAL

Supplementary material for this article is available at http://dmm.biologists.org/lookup/suppl/doi:10.1242/dmm.006775/-/DC1

REFERENCES

Baker, J., Liu, J. P., Robertson, E. J. and Efstratiadis, A. (1993). Role of insulin-like growth factors in embryonic and postnatal growth. *Cell* **75**, 73-82.

Ballard, F. J., Francis, G. L., Ross, M., Bagley, C. J., May, B. and Wallace, J. C. (1987). Natural and synthetic forms of insulin-like growth factor-1 (IGF-1) and the potent derivative, destripeptide IGF-1: biological activities and receptor binding. *Biochem. Biophys. Res. Commun.* **149**, 398-404.

Ballard, F. J., Ross, M., Upton, F. M. and Francis, G. L. (1988). Specific binding of insulin-like growth factors 1 and 2 to the type 1 and type 2 receptors respectively. *Biochem. J.* **249**, 721-726.

Ballard, F. J., Knowles, S. E., Walton, P. E., Edson, K., Owens, P. C., Mohler, M. A. and Ferraiolo, B. L. (1991). Plasma clearance and tissue distribution of labelled insulin-like growth factor-I (IGF-I), IGF-II and des(1-3)IGF-I in rats. *J. Endocrinol.* **128**, 197-204.

Bastian, S. E., Walton, P. E., Wallace, J. C. and Ballard, F. J. (1993). Plasma clearance and tissue distribution of labelled insulin-like growth factor-I (IGF-I) and an analogue LR3IGF-I in pregnant rats. *J. Endocrinol.* **138**, 327-336.

Baxter, R. C. (2000). Insulin-like growth factor (IGF)-binding proteins: interactions with IGFs and intrinsic bioactivities. *Am. J. Physiol. Endocrinol. Metab.* **278**, E967-E976.

Baxter, R. C. and Martin, J. L. (1989). Structure of the Mr 140,000 growth hormone-dependent insulin-like growth factor binding protein complex: determination by reconstitution and affinity-labeling. *Proc. Natl. Acad. Sci. USA* **86**, 6898-6902.

Bayne, M. L., Applebaum, J., Underwood, D., Chicchi, G. G., Green, B. G., Hayes, N. S. and Cascieri, M. A. (1989). The C region of human insulin-like growth factor (IGF) I is required for high affinity binding to the type 1 IGF receptor. *J. Biol. Chem.* **264**, 11004-11008.

Butterfield, G. E., Thompson, J., Rennie, M. J., Marcus, R., Hintz, R. L. and Hoffman, A. R. (1997). Effect of rhGH and rhIGF-I treatment on protein utilization in elderly women. *Am. J. Physiol.* **272**, E94-E99.

Chen, J. W., Ledet, T., Orskov, H., Jessen, N., Lund, S., Whittaker, J., De Meyts, P., Larsen, M. B., Christiansen, J. S. and Frystyk, J. (2003). A highly sensitive and specific assay for determination of IGF-I bioactivity in human serum. *Am. J. Physiol. Endocrinol. Metab.* **284**, E1149-E1155.

Cooke, R. M., Harvey, T. S. and Campbell, I. D. (1991). Solution structure of human insulin-like growth factor **1**, a nuclear magnetic resonance and restrained molecular dynamics study. *Biochemistry* **30**, 5484-5491.

Coolican, S. A, Samuel, D. S., Ewton, D. Z., McWade, F. J. and Florini, J. R. (1997). The mitogenic and myogenic actions of insulin-like growth factors utilize distinct signaling pathways. *J. Biol. Chem.* **272**, 6653-6662.

Courtland, H. W., Demambro, V., Maynard, J., Sun, H., Elis, S., Rosen, C. and Yakar, S. (2010). Sex-specific regulation of body size and bone slenderness by the acid labile subunit. *J. Bone Miner. Res.* **25**, 2059-2068.

Crist, D. M. and Hill, J. M. (1990). Diet and insulinlike growth factor I in relation to body composition in women with exercise-induced hypothalamic amenorrhea. *J. Am. Coll. Nutr.* **9**, 200-204.

Domene, H. M., Bengolea, S. V., Martinez, A. S., Ropelato, M. G., Pennisi, P., Scaglia, P., Heinrich, J. J. and Jasper, H. G. (2004). Deficiency of the circulating insulin-like growth factor system associated with inactivation of the acid-labile subunit gene. *N. Engl. J. Med.* **350**, 570-577.

Domene, H. M., Hwa, V., Argente, J., Wit, J. M., Camacho-Hubner, C., Jasper, H. G., Pozo, J., van Duyvenvoorde, H. A., Yakar, S., Fofanova-Gambetti, O. V. et al. (2009). Human acid-labile subunit deficiency: clinical, endocrine and metabolic consequences. *Horm. Res.* **72**, 129-141.

Flint, D. J., Tonner, E., Beattie, J. and Gardner, M. (1994). Several insulin-like growth factor-I analogues and complexes of insulin-like growth factors-I and -II with insulin-like growth factor-binding protein-3 fail to mimic the effect of growth hormone upon lactation in the rat. *J. Endocrinol.* **140**, 211-216.

Forbes, K. and Westwood, M. (2008). The IGF axis and placental function. a mini review. *Horm. Res.* **69**, 129-137.

Francis, G. L., McMurtry, J. P., Johnson, R. J. and Ballard, F. J. (1990). Plasma clearance of chicken and human insulin-like growth factor-I and their association with circulating binding proteins in chickens. *J. Endocrinol.* **124**, 361-370.

Frystyk, J. (2005). Aging somatotropic axis: mechanisms and implications of insulin-like growth factor-related binding protein adaptation. *Endocrinol. Metab. Clin. North Am.* **34**, 865-876, viii.

Gillespie, C., Read, L. C., Bagley, C. J. and Ballard, F. J. (1990). Enhanced potency of truncated insulin-like growth factor-I (des(1-3)IGF-I) relative to IGF-I in lit/lit mice. *J. Endocrinol.* **127**, 401-405.

Hadsell, D. L., Greenberg, N. M., Fligger, J. M., Baumrucker, C. R. and Rosen, J. M. (1996). Targeted expression of des(1-3) human insulin-like growth factor I in transgenic mice influences mammary gland development and IGF-binding protein expression. *Endocrinology* **137**, 321-330.

Jepsen, K. J., Hu, B., Tommasini, S. M., Courtland, H. W., Price, C., Terranova, C. J. and Nadeau, J. H. (2007). Genetic randomization reveals functional relationships among morphologic and tissue-quality traits that contribute to bone strength and fragility. *Mamm. Genome* **18**, 492-507.

Kaaks, R. (2004). Nutrition, insulin, IGF-1 metabolism and cancer risk: a summary of epidemiological evidence. *Novartis Found. Symp.* **262**, 247-260; discussion 260-268.

King, R., Wells, J. R., Krieg, P., Snoswell, M., Brazier, J., Bagley, C. J., Wallace, J. C., Ballard, F. J., Ross, M. and Francis, G. L. (1992). Production and characterization of recombinant insulin-like growth factor-I (IGF-I) and potent analogues of IGF-I, with Gly or Arg substituted for Glu3, following their expression in Escherichia coli as fusion proteins. *J. Mol. Endocrinol.* **8**, 29-41.

Kreitschmann-Andermahr, I., Suarez, P., Jennings, R., Evers, N. and Brabant, G. (2010). GH/IGF-I regulation in obesity-mechanisms and practical consequences in children and adults. *Horm. Res. Paediatr.* **73**, 153-160.

Lemmey, A. B., Martin, A. A., Read, L. C., Tomas, F. M., Owens, P. C. and Ballard, F. J. (1991). IGF-I and the truncated analogue des-(1-3)IGF-I enhance growth in rats after gut resection. *Am. J. Physiol.* **260**, E213-E219.

Liu, J. L., Grinberg, A., Westphal, H., Sauer, B., Accili, D., Karas, M. and LeRoith, D. (1998). Insulin-like growth factor-I affects perinatal lethality and postnatal development in a gene dosage-dependent manner: manipulation using the Cre/loxP system in transgenic mice. *Mol. Endocrinol.* **12**, 1452-1462.

Liu, P., Jenkins, N. A. and Copeland, N. G. (2003). A highly efficient recombineering-based method for generating conditional knockout mutations. *Genome Res.* **13**, 476-484.

Mathews, L. S., Hammer, R. E., Behringer, R. R., D'Ercole, A. J., Bell, G. I., Brinster, R. L. and Palmiter, R. D. (1988). Growth enhancement of transgenic mice expressing human insulin-like growth factor I. *Endocrinology* **123**, 2827-2833.

McCusker, R. H., Kaleko, M. and Sackett, R. L. (1998). Multivalent cations and ligand affinity of the type 1 insulin-like growth factor receptor on P2A2-LISN muscle cells. *J. Cell Physiol.* **176**, 392-401.

Mohan, S. and Baylink D. J. (2002). IGF-binding proteins are multifunctional and act via IGF-dependent and -independent mechanisms. *J. Endocrinol.* **175**, 19-31.

Ning, Y., Schuller, A. G., Bradshaw, S., Rotwein, P., Ludwig, T., Frystyk, J. and Pintar, J. E. (2006). Diminished growth and enhanced glucose metabolism in triple knockout mice containing mutations of insulin-like growth factor binding protein-3, -4, and -5. *Mol. Endocrinol.* **20**, 2173-2186.

Pennisi, P., Gavrilova, O., Setser-Portas, J., Jou, W., Santopietro, S., Clemmons, D., Yakar, S. and LeRoith, D. (2006). Recombinant human insulin-like growth factor-I treatment inhibits gluconeogenesis in a transgenic mouse model of type 2 diabetes mellitus. *Endocrinology* **147**, 2619-2630.

Ross, M., Francis, G. L., Szabo, L., Wallace, J. C. and Ballard, F. J. (1989). Insulin-like growth factor (IGF)-binding proteins inhibit the biological activities of IGF-1 and IGF-2 but not des-(1-3)-IGF-1. *Biochem. J.* **258**, 267-272.

Sato, A., Nishimura, S., Ohkubo, T., Kyogoku, Y., Koyama, S., Kobayashi, M., Yasuda, T. and Kobayashi, Y. (1993). Three-dimensional structure of human insulin-like growth factor-I (IGF-I) determined by 1H-NMR and distance geometry. *Int. J. Pept. Protein Res.* **41**, 433-440.

Stratikopoulos, E., Szabolcs, M., Dragatsis, I., Klinakis, A. and Efstratiadis, A. (2008). The hormonal action of IGF1 in postnatal mouse growth. *Proc. Natl. Acad. Sci. USA* **105**, 19378-19383.

Sun, B. F., Kobayashi, H., Le, N., Yoo, T. M., Drumm, D., Paik, C. H., McAfee, J. G. and Carrasquillo, J. A. (1997). Biodistribution of 125I-labeled des(1-3) insulin-like growth factor I in tumor-bearing nude mice and its in vitro catabolism. *Cancer Res.* **57**, 2754-2759.

Szabo, L., Mottershead, D. G., Ballard, F. J. and Wallace, J. C. (1988). The bovine insulin-like growth factor (IGF) binding protein purified from conditioned medium requires the N-terminal tripeptide in IGF-1 for binding. *Biochem. Biophys. Res. Commun.* **151**, 207-214.

Thompson, J. L., Butterfield, G. E., Marcus, R., Hintz, R. L., Van Loan, M., Ghiron, L. and Hoffman, A. R. (1995). The effects of recombinant human insulin-like growth factor-I and growth hormone on body composition in elderly women. *J. Clin. Endocrinol. Metab.* **80**, 1845-1852.

Wakai, K., Suzuki, K., Ito, Y., Watanabe, Y., Inaba, Y., Tajima, K., Nakachi, K. and Tamakoshi, A. (2009). Time spent walking or exercising and blood levels of insulin-like growth factor-I (IGF-I) and IGF-binding protein-3 (IGFBP-3): a large-scale cross-sectional study in the Japan Collaborative Cohort study. *Asian Pac. J. Cancer Prev.* **10 Suppl**, 23-27.

Woods, K. A., Camacho-Hubner, C., Savage, M. O. and Clark, A. J. (1996). Intrauterine growth retardation and postnatal growth failure associated with deletion of the insulin-like growth factor I gene. *N. Engl. J. Med.* **335**, 1363-1367.

Yakar, S., Liu, J. L., Fernandez, A. M., Wu, Y., Schally, A. V., Frystyk, J., Chernausek, S. D., Mejia, W. and Le Roith, D. (2001). Liver-specific igf-1 gene deletion leads to muscle insulin insensitivity. *Diabetes* **50**, 1110-1118.

Yakar, S., Rosen, C. J., Beamer, W. G., Ackert-Bicknell, C. L., Wu, Y., Liu, J. L., Ooi, G. T., Setser, J., Frystyk, J., Boisclair, Y. R. et al. (2002a). Circulating levels of IGF-1 directly regulate bone growth and density. *J. Clin. Invest.* **110**, 771-781.

Yakar, S., Wu, Y., Setser, J. and Rosen, C. J. (2002b). The role of circulating IGF-I: lessons from human and animal models. *Endocrine* **19**, 239-248.

Yakar, S., Setser, J., Zhao, H., Stannard, B., Haluzik, M., Glatt, V., Bouxsein, M. L., Kopchick, J. J. and LeRoith, D. (2004). Inhibition of growth hormone action improves insulin sensitivity in liver IGF-1-deficient mice. *J. Clin. Invest.* **113**, 96-105.

Yakar, S., Kim, H., Zhao, H., Toyoshima, Y., Pennisi, P., Gavrilova, O. and LeRoith, D. (2005a). The growth hormone-insulin like growth factor axis revisited: lessons from IGF-1 and IGF-1 receptor gene targeting. *Pediatr. Nephrol.* **20**, 251-254.

Yakar, S., Leroith, D. and Brodt, P. (2005b). The role of the growth hormone/insulin-like growth factor axis in tumor growth and progression: Lessons from animal models. *Cytokine Growth Factor Rev.* **16**, 407-420.

Yakar, S., Bouxsein, M. L., Canalis, E., Sun, H., Glatt, V., Gundberg, C., Cohen, P., Hwang, D., Boisclair, Y., Leroith, D. et al. (2006). The ternary IGF complex influences postnatal bone acquisition and the skeletal response to intermittent parathyroid hormone. *J. Endocrinol.* **189**, 289-299.

Yakar, S., Canalis, E., Sun, H., Mejia, W., Kawashima, Y., Nasser, P., Courtland, H. W., Williams, V., Bouxsein, M., Rosen, C. et al. (2009a). Serum IGF-1 determines skeletal strength by regulating subperiosteal expansion and trait interactions. *J. Bone Miner. Res.* **24**, 1481-1492.

Yakar, S., Rosen, C. J., Bouxsein, M. L., Sun, H., Mejia, W., Kawashima, Y., Wu, Y., Emerton, K., Williams, V., Jepsen, K. et al. (2009b). Serum complexes of insulin-like growth factor-1 modulate skeletal integrity and carbohydrate metabolism. *FASEB J.* **23**, 709-719.